

Electron transfer chemistry of octadecylamine-functionalized single-walled carbon nanotubes

Yiyun Yang^a, Shaowei Chen^{a,*}, Qinbin Xue^b, Alexandru Biris^b, Wei Zhao^{b,*}

^a Department of Chemistry and Biochemistry, University of California, Santa Cruz, CA 95064, USA

^b Department of Chemistry, University of Arkansas, Little Rock, AR 72204, USA

Received 28 July 2004; received in revised form 10 September 2004; accepted 14 September 2004

Available online 7 April 2005

Abstract

Single-walled carbon nanotubes were chemically functionalized by virtue of the interactions between the nanotube-bound carboxylic moieties and octadecylamine ligands. The electronic conductivity properties of the resulting nanotubes were probed voltammetrically. Two approaches were employed. The first entailed the fabrication of a nanotube monolayer at the air|water interface and the conductivity was measured in situ with a vertically aligned interdigitated arrays (IDAs) electrode. The overall current profiles are analogous to those of a Coulomb blockade and the conducting current pathways are found to be one-dimensional within the two-dimensional arrays of nanotubes. The second technique was taking advantage of the dispersibility of the nanotubes in a solution where conventional electrochemical methods were used. From these measurements, the nanotube bandgap energy could also be estimated, which was quite comparable to that determined by spectroscopic measurements.

© 2005 Elsevier Ltd. All rights reserved.

Keywords: Carbon nanotube; Langmuir; Voltammetric; Coulomb blockade; Bandgap

1. Introduction

Ever since the discovery by Iijima in 1991 [1], carbon nanotubes have attracted extensive research interests, as these novel one-dimensional (1D) nanostructures exhibit great potential for applications as the structural elements for molecular-scale devices as well as for optoelectronic nanomachines [2–5]. Single-walled carbon nanotubes (SWNTs) represent a unique class of these 1D nanomaterials with distinct electronic and spectroscopic properties depending on their geometric configurations [2d–f]. However, SWNTs tend to self-assemble into partially ordered two-dimensional bundles [6], rendering it difficult to characterize and correlate the structure and property of individual tubes. Thus, there have been substantial research efforts geared towards the dispersion and processing of these unique carbon materials. Of these, chemical functionalization of nanotubes

has been found to be an effective route towards the dispersion of individual nanotubes where a wide variety of solution-based spectroscopic techniques now become accessible [7,8]. In addition, the dissolved nanotubes can be subject to further chemical and physical manipulations for the fabrication of more complicated functional materials.

One major area of potential applications of SWNTs is as the building blocks for the development of novel electronic nanodevices and sensors [5,9,10]. Therefore, an understanding of the intrinsic electronic conductivity of the nanotubes is of fundamental importance in which electrochemical methods play an important role. So far, in most studies, a relatively thick film of SWNTs was prepared by dropcasting a nanotube solution or suspension onto the electrode surface, and the corresponding voltammetric currents were measured [11–13]. In a more recent study [14], carbon nanotubes were chemically functionalized through the attachments of pyrrolidines to the external wall and the resulting nanotubes were dissolved into an electrolyte solution where the voltammetric properties were probed similarly to those of conventional redox molecules. One key conclusion is that while surface

* Corresponding authors. Fax: +1 831 459 2935.

E-mail addresses: schen@chemistry.ucsc.edu (S. Chen), wz Zhao@ualr.edu (W. Zhao).

chemical functionalization did modify the electronic states of pristine nanotubes, the overall electronic density of states was not strongly affected, and the nanotube metallic characters were (at least partly) retained. This paves the way to the investigation of nanotube bulk electronic properties by using chemically functionalized and dispersible nanotubes.

In this article, we report the electrochemical and spectroscopic studies of surfactant-functionalized single-walled carbon nanotubes. Two electrochemical approaches are used and the results are compared to those by spectroscopic measurements. The first entails voltammetric current measurements with the SWNTs dissolved in organic media while the other is a solid-state based technique. In the latter approach, a monolayer of nanotubes is prepared on the water surface by the Langmuir method and the electronic conductivity properties of the nanotube film are examined by a vertically aligned interdigitated arrays (IDA) electrode at the air|water interface where the corresponding current–potential (I – V) responses are collected in situ. Recently, we have used this solid-state method to investigate the electronic conductivity of various metal and semiconductor nanoparticles [15–17]. We found that the interparticle interactions as well as photoexcitation are two important variables that could be exploited to manipulate the electron-transfer chemistry across the particle monolayer. Similar but more complicated behaviors are observed when this method is extended to 1D nanomaterials such as SWNTs primarily because of the structural anisotropy and dispersities of the nanotube dimension and aspect ratio, as detailed below.

2. Experimental

2.1. Materials

The octadecylamine (ODA)-SWNTs were prepared by following a literature protocol developed by the Haddon group [18]. The reaction is basically an acid–base reaction where ODA reacts with carboxylic-functionalized SWNTs (SWNTs-COOH) to form ODA-SWNT-carboxylate ion pairs. The typical length of the SWNTs is 200–1600 nm with the diameter of 1.4 nm. The reaction was carried out by heating nitric acid-treated SWNTs (full-length SWNTs with purity >80% made by an electric-arc technique and purchased from Carbon Solutions Inc.) in neat ODA (97%, from Aldrich) at 85 °C for 6 days. Thermogravimetric analysis (TGA) indicated about 60 wt.% of ODA in the resulting ODA-SWNTs. While the ODA ligands are primarily ionically bound to the ends and defect sites of the nanotubes, there may be some ODA molecules that are physically adsorbed onto the sidewall [18b].

2.2. Spectroscopies

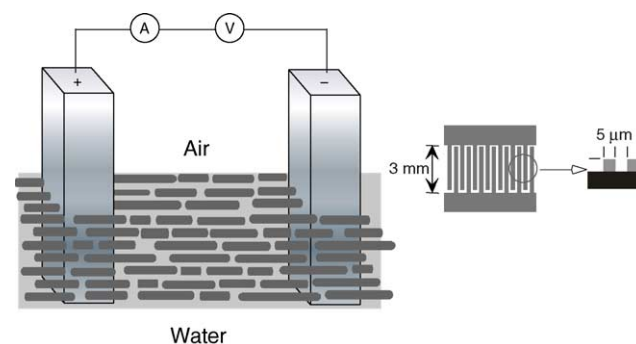
For AFM measurements, the samples were prepared on mica substrates and were scanned in tapping mode by a

Digital Instruments Dimension 3100 AFM Nanoscope. The scanned area was 10 μm^2 at a scan rate of 1.98 Hz. The tips used were RTESP Si_3N_4 with a length of 125 μm and vibrating at a frequency of 300 kHz. It should be noted that from AFM measurements, along with these SWNTs, there are also a number of carbon particles present in the sample (not shown). However, elemental analysis by energy-dispersive X-ray (EDX) analysis did not show the presence of any element other than carbon indicating a rather complete removal of the metal catalysts used in the nanotube synthesis.

UV–vis–NIR absorption spectra of the ODA-SWNTs in tetrahydrofuran (THF) were acquired by using a Perkin-Elmer UV/Vis/NIR Lambda 19 spectrometer. A quartz cuvette of 1 mm path length was used in the experiment. The nanotube concentration was about 0.2 mg/mL and the solvent THF was used as the reference for background subtraction.

2.3. Solid-state voltammetry

In a typical measurement, a monolayer of nanotubes was formed at the air|water interface using the Langmuir technique (NIMA 611D). Generally 110 μL of the nanotube solutions (0.33 mg/mL CHCl_3) was spread dropwise onto the water surface (water supplied by a Barnstead Nanopure water system, $\geq 18 \text{ M}\Omega$). At least 20 min was allowed for solvent evaporation as well as between compression cycles. An interdigitated arrays (IDA, from ABTECH Scientific) electrode was aligned vertically at the air|water interface where a monolayer of nanotubes was trapped between the IDA fingers (details of the experimental setup was shown in Scheme 1, as described previously [15–17]). The IDA electrode consists of 25 pairs of gold fingers with dimensions of 3 mm \times 5 μm \times 5 μm ($L \times W \times H$). The corresponding current–potential (I – V) profiles were collected directly at the air|water interface by applying a voltage bias to the contacts of the finger pairs using an EG&G PARC Potentiostat (model 283) and EG&G commercial software (PowerCV[®] and PowerPulse[®]).



Scheme 1. Experimental setup for electronic conductivity measurements at the air|water interface. Note that actual arrangements of the nanotubes are unknown and surfactant ligands are omitted for the sake of clarity. Inset shows the geometric configuration of the IDA electrode.

2.4. Electrochemistry

Electrochemical measurements were carried out with a CHI 440 Electrochemical workstation. A polycrystalline gold disk electrode (0.0152 cm^2) sealed in a glass tubing was used as the working electrode, a Ag/AgCl as the reference and a Pt coil as the counter electrode. Prior to electrochemical measurements, the Au electrode was polished with $0.05 \mu\text{m}$ $\alpha\text{-Al}_2\text{O}_3$ slurries (Buehler), followed by extensive rinsing with dilute H_2SO_4 , nanopure water, ethanol, and acetone, consecutively. The nanotubes were dissolved in dry THF and the solution was deaerated with ultra-high-purity nitrogen (Airgas) for at least 20 min and blanketed with a nitrogen atmosphere during the entire experimental procedure.

3. Results and discussion

3.1. Solid-state electronic conductivity

Fig. 1 shows the Langmuir isotherm of the nanotube monolayer at the air|water interface. One can see that the take-off area is about 280 cm^2 (corresponding to ca. $7.71 \times 10^3 \text{ cm}^2/\text{mg}$ of SWNTs). At surface area larger than 280 cm^2 , the nanotube layer is equivalent to a two-dimensional gas where intertube interaction is relatively weak; whereas at smaller surface area, the surface pressure increases quite rapidly, which indicates that the nanotubes are now in contact with each other, most likely resulting in the intercalation of the ODA ligands. The overall behaviors are quite similar to those of alkanethiolate-protected nanoparticles [15–17,19].

The corresponding electronic conductivity properties of the nanotube monolayers are then probed voltammetrically at varied surface pressures (and hence intertube separations)

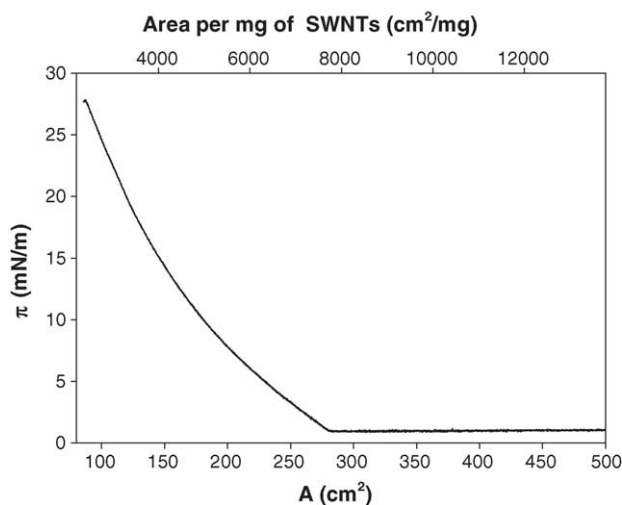


Fig. 1. Langmuir isotherm of an ODA-SWNT monolayer at the air|water interface. Nanotube solution was prepared at a concentration of 0.33 mg/mL in CHCl_3 . Solution spread $110 \mu\text{L}$. Compression barrier speed $10 \text{ cm}^2/\text{min}$.

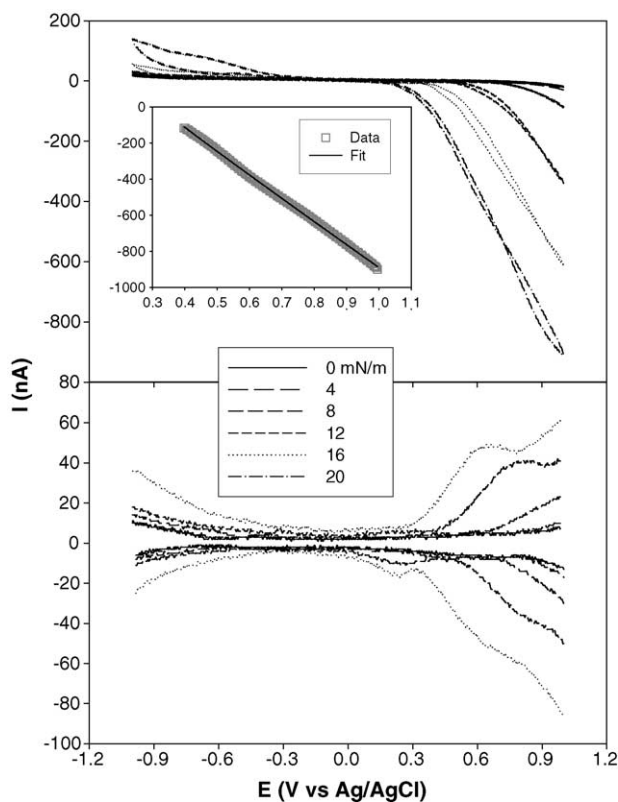


Fig. 2. Cyclic voltammograms (CV, upper panel) and differential pulse voltammograms (DPV, lower panel) of an ODA-SWNT monolayer at the air|water interface. The corresponding surface pressures are shown in figure legends. In CV, potential sweep rate 100 mV/s ; in DPV, DC ramp 10 mV/s , pulse amplitude 50 mV . Inset shows the fitting of the cathodic scan current at $E > 0.4 \text{ V}$ (at $\pi = 20 \text{ mN/m}$) by the Coulomb blockade power law, $I = I_0(E/E_T - 1)^5$.

by using a vertically aligned IDA electrode at the air|water interface (Scheme 1). Fig. 2 shows the resulting cyclic (A, CVs) and differential pulse (B, DPVs) voltammograms. First, one can see that with increasing surface pressure (and decreasing intertube separation), the voltammetric currents increase accordingly, which can be attributable to the more efficient electron transfer between neighboring nanotubes because of the shorter tunneling barriers. This effect is much more significant at positive potentials than at negative potentials, i.e., the oxidation step is more sensitive to the intertube interactions than the reduction step; and the consequence is that the overall I - V profile is progressing to that of a molecular diode. In a previous study by quantum chemical calculations [20], Yang et al. showed that the intertube charge transfer is mainly determined by the tube diameter: for larger tubes, hole transport dominates whereas for smaller tubes, electron transport. Thus, one may suspect that, equivalently, at high surface pressures, hole transport becomes the dominating mechanism. This is not surprising given that the nanotubes are mostly hole-doped after the standard purification process [8b].

As the overall current–potential profiles are analogous to that of a Coulomb blockade [15–17], especially at high surface pressures, theory predicts that at sufficiently large poten-

tial ($E > E_T$ with E_T being the threshold potential), the current should scale as a power law, $I = I_0(E/E_T - 1)^\zeta$, where the scaling exponent ζ reflects the accessible current-conducting pathways. For instance, for 1D and 2D (spherical) nanoparticle arrays, both modeling [21] and experiment [22] show ζ to equal approximately the array dimensionality. In a more recent study involving 3D ordered assemblies of gold nanoparticles [23], ζ was found to be close to 3. Fig. 2A inset shows the cathodic scan current (open square) within the potential range of +0.4 and +1.0 V (at $\pi = 20$ mN/m) and the fitting (solid line) by the above equation. One can see that the fitting is excellent ($R^2 = 0.9994$) and ζ is found to be 0.97. An equally good fitting (not shown) can also be found with the anodic scan current within the same potential range ($R^2 = 0.9977$) and ζ is found to be 1.04. These indicate that the effective charge-transfer pathway within the nanotube ensemble is essentially one-dimensional. At first glance, this is somewhat counterintuitive as one might expect a value close to 2 since the nanotubes are in a two-dimensional array. However, in contrast to the “spherical” nanoparticles used in the previous studies [21–23], nanotubes exhibit unique anisotropic structural characteristics; and it has been found that the electronic conductivity along the axis direction is significantly higher than that perpendicular to the tube axis [24]. Thus, within the nanotube monolayer on the water surface, it is reasonable to believe that the most efficient charge transport pathway is along the nanotube axes (in combination with charge hopping between neighboring tubes).

Second, there appears to be a hysteresis of the voltammetric currents at positive potential region (Fig. 2A). Similar behaviors were also observed with alkanethiolate-protected gold nanoparticle monolayer [15], which was ascribed to the electrical field-induced dipole interactions between neighboring nanotubes (the so-called memory effect).

Third, from Fig. 2 one can see that at $E > 0$, the potential at which the current starts to increase seems to shift negatively with increasing surface pressure; whereas at $E < 0$, positively. In our previous study [16] with semiconductor quantum dots, we also observed a similar behavior. It was interpreted on the basis of the shrinkage of the effective bandgap energy with decreasing interdot separation. From DPV measurements (panel B), one can see that the potential shift is more pronounced in the positive potential regime than in the negative counterpart. This suggests that the energy of the valence band (or equivalently, the HOMO band) electrons is more sensitive to nanotube packing and intertube interactions than that of the conduction (or LUMO) electrons, in consistency with the afore-mentioned charge-transfer mechanism dominated by hole transport.

We also examined the effects of photoexcitation by comparing the nanotube electronic conductivity properties when the measurements were carried out in the dark and when the monolayer was exposed to a low-power laser (≤ 25 mW, wavelength 473, 532, or 638 nm) during voltammetric measurements. Typically, we observed a slight enhancement of the voltammetric currents at the positive potential regime

upon photoexcitation whereas virtually no change was found at negative potentials. In addition, the current profiles at positive potentials were also found to shift negatively upon photo perturbation (akin to that shown in Fig. 2). However, turning off the laser did not lead to the recovery of the original conductivity profile, indicating that these two effects were quite irreversible.

While the detailed nanotube arrangements are unknown in the monolayer films [25], the structure most likely mirrors that of logs on a river [26] where at sufficiently high surface pressures the tubes are arranged in a side-by-side configuration (Scheme 1). Certainly because of the dispersity of the nanotube dimensions, aspect ratios, as well as the presence of nanosized particle impurities, the monolayer is not anticipated to be of long-range order. Thus, the voltammetric currents should be best understood as the effective reflection of the bulk electrical conductivity.

3.2. Electron-transfer chemistry in solutions

We also investigated the charge-transfer chemistry of nanotubes dispersed in solutions. Fig. 3 shows some representative cyclic (A, CVs) and differential pulse (B, DPVs) voltammograms of a TBAP solution in dry THF containing ODA-SWNTs at a concentration of 3 mg/mL. It should be noted that

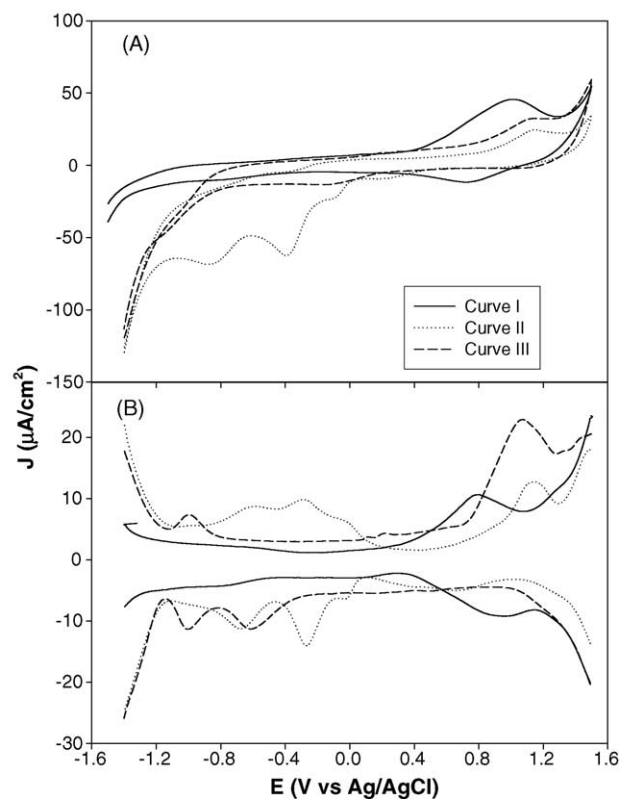


Fig. 3. Cyclic (A, CV) and differential pulse voltammograms (B, DPV) of ODA-SWNT at a gold electrode (0.0152 cm 2) in dried THF containing 0.1 M TBAP. Nanotube concentration 3 mg/mL. In CV: potential sweep rate 100 mV/s; in DPV: DC ramp 10 mV/s, pulse amplitude 50 mV.

the voltammetric responses are rather dynamic and no clear steady state is reached, and the overall behaviors are quite different from those of pyrrolidine-functionalized nanotubes in THF [14]. The behaviors can be divided into at least three representative stages. Curve I reflects the initial response. One can see that there is a pair of broad peaks at ca. +0.9 V with a peak splitting (ΔE_p) of about 0.2 V, indicating a quasi-reversible charge-transfer process. This might be ascribed to the oxidation of the nanotubes (for instance, the defect sites that have not been oxidized in the nitric acid reaction). One may also argue that this arises from the oxidation of the amine moieties (of the ODA layer) into radical cations. However, electro-oxidation of primary amine has generally been found to occur at much more positive potentials [27]. In addition, typically the resulting radical species are not stable and tend to attach to the electrode surface through a metal–C covalent bond [27]. Consequently, one would observe a diminishing of the electrode double-layer charging. However, we did not see this in our study (Fig. 2 and *vide infra*), thus it is unlikely that this voltammetric feature is due to electro-oxidation of the ODA amine moieties.

In contrast, within the potential range of +0.4 to –1.5 V, the response is virtually featureless. In a previous study involving dropcast films of SWNTs [13], it was found that in dry and aprotic media, the main contribution to the voltammetric currents was the capacitive charging to the electrode double layer, which was featureless in nature.

However, repetitive cycling of potentials lead to the evolution of the voltammetric responses into the next stage which is represented by curve II. Here one can see that the oxidation peak shifts to slightly more positive potentials and becomes more irreversible without an apparent cathodic return wave. Concurrently, at least three pairs of voltammetric peaks start to emerge in the negative potential regime at –0.03, –0.27, and –0.60 V. Some analogous features were also observed with SWNT dropcast films onto a gold electrode surface which were ascribed to the electro-reduction of the nanotube carbonyl moieties (C=O) in the presence of trace of water [11,13].

With continued potential cycling, the voltammetric responses exhibit further variation (curve III). While the oxidation peak appears to be virtually unchanged in terms of the peak potential, the reduction peaks show quite a drastic shift in the cathodic direction. A cathodic peak can now be found at –0.6 V without an anodic return wave, and a second pair of peaks at –1.0 V. These seem to suggest that the electro-reduction of the nanotube carbonyl moieties has now to overcome a rather substantial overpotential, which might be related to the spatial distribution of C=O on the nanotube surface.

Overall, one can see that the electro-oxidation of ODA-SWNTs is more active than the reduction step which seems to require an induction time (curve II). This is in agreement with the solid-state voltammetric study in Section 1. However, the detailed origin of these electrochemical features is not clear at the moment and further work is desired.

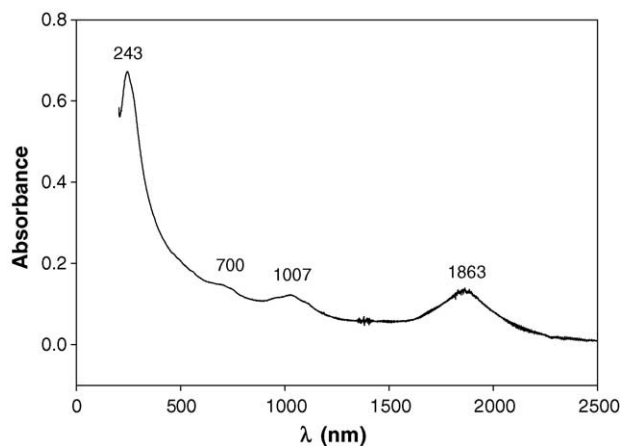


Fig. 4. UV-vis-NIR spectrum of ODA-SWNTs dissolved in THF at a concentration of about 0.2 mg/mL.

3.3. Spectroscopy

The ODA-SWNTs used in the above electrochemical studies were also subject to spectroscopic characterizations. Fig. 4 shows the UV-vis-NIR spectrum of ODA-SWNTs dispersed in dry THF at a concentration of 0.2 mg/mL (contributions from surfactant and solvent have been subtracted as background). One can see that there are four major absorption peaks at 243, 700, 1007, and 1863 nm. These peaks are assigned to SWNTs, uniquely, based on extensive experimental measurements which match theoretical calculations [8]. No absorption band is observed for the surfactant ligands within the same wavelength range. The peaks at 1863 nm (0.67 eV) and 1007 nm are ascribed to the first (bandgap energy) and second interband transition, respectively, of the semiconducting SWNTs present in the sample [8]. The absorption feature at 700 nm is the first interband transition of metallic SWNTs [8b]; and the 243 nm feature is assigned to π -plasmon absorption [8b]. These features indicate that metallic and semiconducting nanotubes are both present in the sample. We did not, however, observe any fluorescence emission within the visible range.

Previously, we have shown that voltammetric measurements could also serve as a complementary and comparable method in the evaluation of nanomaterial bandgap energy [16,28]. From the above solid-state electrochemical studies, one can estimate the effective bandgap energy of the nanotubes to be >0.8 eV (at 16 mN/m, Fig. 2) [29], based on the width of the central potential gap [16,28]. One might note that the bandgap energy evaluated from spectroscopic measurements is somewhat smaller than that determined by the above voltammetric results. In electrochemical measurements, the effective bandgap energy will be primarily determined by the largest bandgap available in the ensemble as they are the limiting factor of the overall electronic conductivity properties; additionally, the disorder and defects within the SWNT ensemble will also lead to a decrease in electronic conductivity and hence equivalently an increase

in the bandgap energy. By contrast, in spectroscopic measurements, the effective bandgap is estimated by the corresponding peak energies whose widths reflect a distribution of the nanotubes with varied structures and electronic energies.

4. Conclusions

Chemical functionalization renders single-walled carbon nanotubes dispersible in solutions. Electrochemical studies demonstrate that in solid state, the ensemble charge transfer is dominated by hole transport, which is increasingly pronounced at small intertube separation. In addition, the accessible conducting current pathways are found to be one-dimensional within the two-dimensional nanotube ensemble, most probably arising from the anisotropic nature of the nanotube structure, in contrast to (isotropic) spherical nanoparticles. Solution electrochemistry shows that the oxidation step is more active than the reduction counterpart and a dynamic transition is observed where the voltammetric responses might arise from the Faradaic pseudocapacitive charging of the nanotube molecules. Importantly, the bandgap energies of the nanotube ensemble can be evaluated from both voltammetric and spectroscopic measurements which show rather comparable results.

In the current study, a rather polydisperse sample (mixture of both metallic and semiconducting SWNTs, along with carbon particle contaminants) was used. Nonetheless, the results reported herein will serve as a starting point in our continued pursuit of understanding the electronic conductivity properties of bulk nanotube materials. We are currently working on the further purification of the SWNTs and the results will be reported in due course.

Acknowledgments

This work was supported, in part, by the National Science Foundation (CAREER Award CHE-0092760, S.C.), the ACS—Petroleum Research Fund (S.C.) and the University of California—Santa Cruz (S.C.). S.C. is a Cottrell Scholar of the Research Corporation. W.Z. acknowledges financial support from the ARO under Award No. DAAD 190210140.

References

- [1] S. Iijima, *Nature* 354 (1991) 56.
- [2] (a) M. Ouyang, J. Huang, C.M. Lieber, *Acc. Chem. Res.* 35 (2002) 1018;
(b) P. Avouris, *Acc. Chem. Res.* 35 (2002) 1026;
(c) H. Dai, *Acc. Chem. Soc.* 35 (2002) 1035;
(d) O. Zhou, H. Shimoda, B. Gao, S. Oh, L. Fleming, G. Yue, *Acc. Chem. Soc.* 35 (2002) 1045;
(e) M.S. Dresselhaus, G. Dresselhaus, A. Jorio, A.G. Souza Filho, M.A. Pimenta, R. Saito, *Acc. Chem. Res.* 35 (2002) 1070;
(f) J.E. Fischer, *Acc. Chem. Res.* 35 (2002) 1079;
(g) S. Niyogi, M.A. Hamon, H. Hu, B. Zhao, P. Bhowmik, R. Sen, M.E. Itkis, R.C. Haddon, *Acc. Chem. Res.* 35 (2002) 1105.
- [3] M. Ouyang, J. Huang, C.M. Lieber, *Annu. Rev. Phys. Chem.* 53 (2002) 201.
- [4] Z. Yao, H.W.C. Postma, L. Balents, C. Dekker, *Nature* 402 (1999) 273.
- [5] Y. Lin, F. Lu, Y. Tu, Z. Ren, *Nano Lett.* 4 (2004) 191.
- [6] A. Thess, R.S. Lee, P. Nikolaev, H. Dai, P. Petit, J. Robert, C. Xu, H. Lee, S.G. Kim, D.T. Colbert, G. Scuseria, D. Tomanek, J.E. Fischer, R.E. Smalley, *Science* 273 (1996) 483.
- [7] Y. Sun, K. Fu, Y. Lin, W. Huang, *Acc. Chem. Res.* 35 (2002) 1096.
- [8] (a) J. Chen, M.A. Hamon, H. Hu, Y. Chen, A.M. Rao, P.C. Eklund, R.C. Haddon, *Science* 282 (1998) 95;
(b) M.E. Itkis, S. Niyogi, M.E. Meng, M.A. Hamon, H. Hu, R.C. Haddon, *Nano Lett.* 2 (2002) 155;
(c) W. Zhao, C. Song, P.E. Pehrsson, *J. Am. Chem. Soc.* 124 (2002) 12418;
(d) C. Dekker, *Phys. Today* 52 (1999) 22.
- [9] J. Hahn, C.M. Lieber, *Nano Lett.* 4 (2004) 51.
- [10] A. Javey, Q. Wang, A. Ural, Y. Li, H. Dai, *Nano Lett.* 2 (2002) 929.
- [11] H. Luo, Z. Shi, N. Li, Z. Gu, Q. Zhuang, *Anal. Chem.* 73 (2001) 915.
- [12] C. Stephan, T.P. Nguyen, L. Vaccarini, P. Berier, in: H. Kuzmany (Ed.), *Electronic Properties of Novel Materials—Molecular Nanostructures*, American Institute of Physics, 2000, p. 363.
- [13] (a) L. Kavan, P. Rapta, L. Dunsch, M.J. Bronikowski, P. Willis, R.E. Smalley, *J. Phys. Chem. B* 105 (2001) 10764;
(b) Another possibility is that these three peaks are related to the energy gaps of metallic nanotubes, bundles, and S_{11} transitions [8b].
- [14] M. Melle-Franco, M. Marcaccio, D. Paolucci, F. Paolucci, V. Georgakilas, D.M. Guldi, M. Prato, F. Zerbetto, *J. Am. Chem. Soc.* 126 (2004) 1646.
- [15] S. Chen, *Anal. Chim. Acta* 496 (2003) 29.
- [16] I.A. Greene, F. Wu, J.Z. Zhang, S. Chen, *J. Phys. Chem. B* 107 (2003) 5733.
- [17] Y. Yang, S. Pradhan, S. Chen, *J. Am. Chem. Soc.* 126 (2004) 76.
- [18] (a) J. Chen, A.M. Rao, S. Lyuksyutov, M.E. Itkis, M.A. Hamon, H. Hu, R.W. Cohn, P.C. Eklund, D.T. Colbert, R.E. Smalley, R.C. Haddon, *J. Phys. Chem. B* 105 (2001) 2525;
(b) D. Chattopadhyay, I. Galeska, F. Papadimitrakopoulos, *J. Am. Chem. Soc.* 125 (2003) 3370.
- [19] (a) S. Chen, *J. Phys. Chem. B* 104 (2000) 663;
(b) S. Chen, *Langmuir* 17 (2001) 2878;
(c) S. Chen, *Langmuir* 17 (2001) 6664.
- [20] X. Yang, L. Chen, Z. Shuai, Y. Liu, D. Zhu, *Adv. Funct. Mater.* 14 (2004) 289.
- [21] (a) C.T. Black, C.B. Murray, R.L. Sandstrom, S.H. Sun, *Science* 290 (2000) 1131;
(b) A.A. Middleton, N.S. Winggreen, *Phys. Rev. Lett.* 71 (1993) 3198.
- [22] A.J. Rimberg, T.R. Ho, J. Clarke, *Phys. Rev. Lett.* 74 (1995) 4714.
- [23] H. Fan, K. Yang, D.M. Boye, T. Sigmon, K.J. Malloy, H. Xu, G.P. Lopez, C.J. Brinker, *Science* 304 (2004) 567.
- [24] X. Wang, Y. Liu, G. Yu, C. Xu, J. Zhang, D. Zhu, *J. Phys. Chem. B* 105 (2001) 9422.
- [25] We were unable to observe the nanotube structures with transmission electron microscopy (Hitachi H7100) by depositing an ODA-SWNT monolayer onto a TEM grid using the Langmuir–Blodgett technique most probably because of the low electron density of dispersed nanotubes and the limitation of the instrumental resolution.
- [26] (a) F. Kim, S. Kwan, J. Akana, P. Yang, *J. Am. Chem. Soc.* 123 (2001) 4360;

- (b) P. Yang, F. Kim, *Chem. Phys. Chem.* 3 (2002) 503;
(c) P. Yang, *Nature* 425 (2003) 243.
- [27] A. Adenier, M.M. Chehimi, I. Gallardo, J. Pinson, N. Vilà, *Langmuir* 20 (2004) 8243.
- [28] (a) S. Chen, L.A. Truax, J.M. Sommers, *Chem. Mater.* 12 (2000) 3864;
(b) S.K. Haram, B.M. Quinn, A.J. Bard, *J. Am. Chem. Soc.* 123 (2001) 8860.
- [29] The dynamic behaviors of voltammetric responses in solution electrochemistry (Section 2) made it difficult to have a meaningful evaluation of the nanotube bandgap energy.